

Flagella-Driven Flows Enhance Long-Range Transport of Molecular Nutrients

Martin B. Short^a, Cristian A. Solari^b, Sujoy Ganguly^a, Thomas

R. Powers^c, John O. Kessler^a, and Raymond E. Goldstein^{a,d,e}

^aDepartment of Physics, ^bDepartment of Ecology and Evolutionary Biology,

^dProgram in Applied Mathematics, and ^eBIO5 Institute, University of Arizona, Tucson, AZ 85721 and

^cDivision of Engineering, Box D, Brown University, Providence, RI 02912

Evolution from unicellular organisms to large, multicellular ones requires matching their needs to the rate of exchange of molecular nutrients with the environment. This logistic problem poses a severe constraint on development. For organisms whose body plan is a spherical shell, such as the volvocine green algae, the current of needed nutrients grows quadratically with radius, whereas the rate at which diffusion alone exchanges molecules grows linearly, leading to a bottleneck radius beyond which the diffusive current cannot meet metabolic demands. Using *Volvox carteri*, we examine the role that advection of fluid by the coordinated beating of surface-mounted flagella plays in enhancing nutrient uptake, and show that it generates a boundary layer of concentration of the diffusing solute. That concentration gradient produces an exchange rate which is quadratic in the radius, as required, thus circumventing the bottleneck and allowing increase in size and evolutionary transitions featuring germ-soma differentiation.

The motility of microorganisms is primarily thought to enable access to optimum environments. Yet some species of colonial motile algae thrive in restrictive habitats such as shallow evanescent puddles, all the while paddling energetically with their flagella. What is the significance, beyond locomotion, of this collective coordinated beating of flagella? Algal metabolism requires exchange, between organisms and water, of small molecules and ions such as CO₂, O₂, and phosphate. Rapidly growing organisms that are “large” in the sense explained below, must augment diffusion with effective modes of transport from remote reaches of their environment.¹ The volvocine green algae^{2–5} can serve as a model system for understanding how exchange of nutrients and wastes varies with organism size, as in the transition from unicellular to ever larger multicellular colonies. The Volvocales range from the unicellular *Chlamydomonas* to large colonies of cells, eventually leading to *Volvox*, comprising 1,000–50,000 cells (Fig. 1). They include closely related lineages with different degrees of cell specialization in reproductive and vegetative function (germ-soma separation), which seem to represent “alternative stable states.”⁶ Phylogenetic studies show that transitions in cell specialization have occurred multiple times, independently,^{7–9} to geometrically and functionally similar configurations, suggesting that there is a selective advantage to that morphology. The volvocalean range of sizes, over three orders of magnitude, enables the study of scaling laws; from a theoretical perspective, the spherical form of the Volvocales simplifies mathematical analysis.

Volvox, the largest colonies in the lineage, are formed by sterile biflagellated *Chlamydomonas*-like somatic cells, with outwardly oriented flagella, which are embedded at the surface of a transparent extracellular matrix (ECM) that also contains the gonidia (germ cells). Directional swimming due to the coordinated beating of these flagella is also accompanied by rotation, or “rolling,” for

which *Volvox* is named.² Embedded in the ECM inside the colony are the germ cells that develop into daughter colonies. Bell and Koufopanou^{10,11} suggested that the ECM is a storehouse (“source”) of nutrients that diffuse to the germ cells (“sink”). They interpret this source-sink coupling as a mechanism that increases the uptake of nutrients by the developing germ cells located within the colony. It has been shown experimentally^{10,11} that the unflagellated germ cells, when liberated from their mother colony and freely suspended in the growth medium, grow more slowly than those embedded in intact colonies. Those experimental studies did not consider the flow created by collective flagellar beating of the mother colonies. Our recent studies^{3,4} show that these flows can be replaced by externally supplied stirring, which returns germ cells to normal growth rates. Flagella obviously

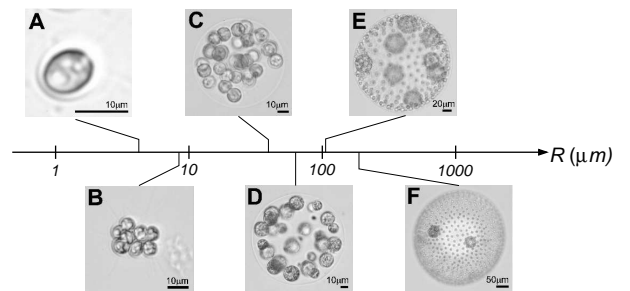


FIG. 1: Volvocine green algae arranged according to typical colony radius R . The lineage ranges from the single-cell *Chlamydomonas reinhardtii* (A), to undifferentiated *Gonium pectorale* (B), *Eudorina elegans* (C), to the soma-differentiated *Pleodorina californica* (D), to the germ-soma differentiated *Volvox carteri* (E), *V. aureus* (F), and even larger (e.g. *V. gigas* with a radius of 1 mm). Where two cell types can be identified, the smaller are somatic cells and the larger are reproductive cells. Note that the number of cells in *Volvox* ranges from 1,000 – 50,000.

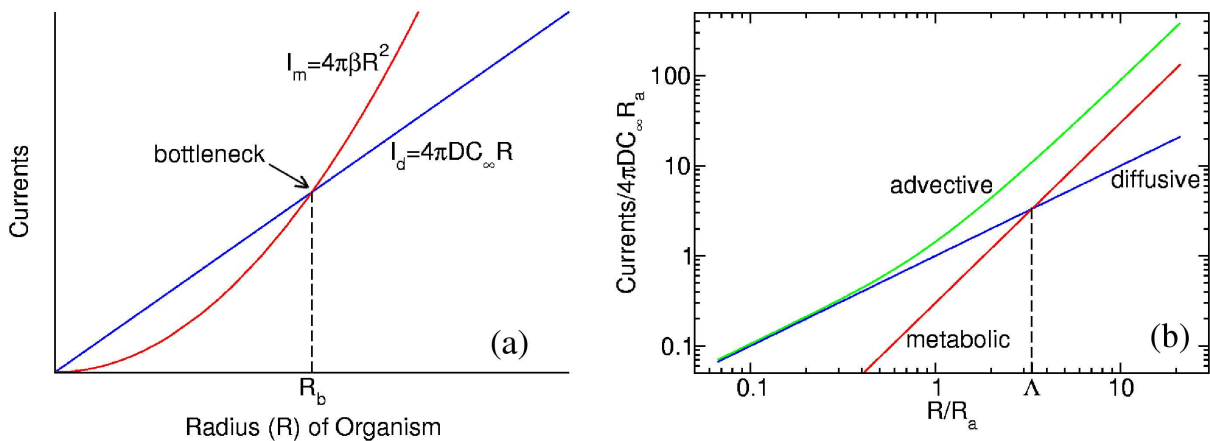


FIG. 2: Molecular currents and requirements. (a) A schematic diagram illustrating the existence of the diffusive bottleneck R_b . When the metabolic demand current (red), which is quadratic in organism radius R , exceeds the diffusive current (blue), which is only linear in R , the organism can no longer survive by diffusion alone. (b) Log-log plot showing how the advective current (green) circumvents the diffusive bottleneck for the choice $\Lambda \equiv R_b/R_a = 3.3$. At radii greater than the advective radius R_a , the advective current grows quadratically with R , allowing metabolic needs to be satisfied for arbitrary size.

confer motility; we infer that they also play a subtle but crucial role in metabolism. Niklas¹ suggested that as organisms increase in size, stirring of boundary layers, yielding transport from remote regions, can be fundamental in maintaining a sufficient rate of metabolite turnover, one not attainable by diffusive transport alone. Yet there has not been a clear quantitative analysis of this putative connection between flagella-driven stirring and nutrient uptake. Here we investigate the hypothesis that those flows facilitate, even “encourage,” the transition to large multicellular forms. We analyze the idealized problem of the scaling that relates nutrient uptake to body size. Measurements of the actual flow fields generated by colonies confirm the analysis. Since we also aim to understand the physical constraints leading to germ-soma differentiation, we investigate a body plan without such differentiation and examine its failure to deal with those constraints.

Results: Bottleneck Radius

Consider the case in which only molecular diffusion in the suspending fluid governs transport (uptake or rejection) of a species whose concentration as a function of radial coordinate r is $C(r)$. When more than even a few percent of the colony surface is covered by an array of absorbers or emitters, the diffusion-limited rate is well-approximated by that of a uniformly covered sphere.¹² We now focus, for simplicity, on nutrient acquisition. If C_∞ is the concentration far from the colony, the steady-state concentration, $C(r) = C_\infty(1 - R/r)$, yields an inward current $I_d = D \int dS (\partial C / \partial r)$ linear in the colony radius R ,

$$I_d = 4\pi DC_\infty R. \quad (1)$$

The timescale τ_D on which this steady-state profile develops from an initially uniform concentration is $\tau_D \simeq$

R^2/D . For a typical colony of radius $200\mu\text{m}$ and diffusion constant of $D = 2 \times 10^{-5} \text{ cm}^2/\text{s}$, $\tau_D \simeq 20 \text{ s}$, which is very long compared to the flagella beat period but short compared to the life cycle. The current (1) can be compared with the metabolic requirements of a colony with surface-mounted cells,

$$I_m = 4\pi R^2 \beta, \quad (2)$$

where β is the time-dependent nutrient demand rate per unit area, including the requirements of (internal) germ cells, and storage into the ECM. The diffusive uptake can exceed the requirements at small radii. At sizes greater than the *bottleneck radius*

$$R_b = \frac{DC_\infty}{\beta}, \quad (3)$$

defined as occurring when $I_d = I_m$, diffusion is insufficient to feed the organism (Fig. 2a). The diffusive rejection of waste products is also limited by a bottleneck radius of the same form as Eq. 3, with β signifying the forced emission rate of waste, and C_∞ replaced by the difference between a molecular waste concentration at the surface and at infinity.

Estimation of the bottleneck radius includes several considerations. First, the demand/consumption rate β varies with time during the life cycle of *Volvox*. Second, that rate may depend on nutrient availability. Third, there is uncertainty as to which of the key nutrients is limiting. Fourth, it is arguable whether the boundary condition for waste rejection at the colony surface involves a specified flux or a concentration. Mindful of these difficulties, we can make a rough estimate using parameters appropriate for either phosphate¹³ ($D \simeq 10^{-5} \text{ cm}^2/\text{s}$, $C_\infty \simeq 6 \times 10^{14} \text{ cm}^{-3}$, and $\beta \simeq 10^{12} \text{ cm}^{-2}\text{s}^{-1}$) or oxygen ($D \simeq 2 \times 10^{-5} \text{ cm}^2/\text{s}$, $C_\infty \simeq 10^{17} \text{ cm}^{-3}$, and

$\beta \simeq 10^{14} \text{ cm}^{-2}\text{s}^{-1}$ measured in *V. carteri* using BOD bottles). We find $R_b \simeq 50\text{--}200 \text{ }\mu\text{m}$. Intriguingly, the low range of the estimated R_b is comparable to *Pleodorina* (Fig. 1D); the high range is comparable to the smallest germ-soma differentiated *Volvox* colonies (e.g., Fig. 1E). Note that *Pleodorina* is considerably smaller than *Volvox*. In the latter, the number of flagellated surface-mounted somatic cells is much higher and germ cells, which are non-flagellated, lie in the interior of the colony.

As a consequence of the dual role played by the flagellar basal bodies as both anchoring points for flagella and as microtubule organizing centers active in cell division, undifferentiated colonies are subject to the ‘‘flagellation constraint,’’^{5,14} which prevents the use of flagella during cell division. It is therefore appropriate that the largest colonies without true germ-soma differentiation would have a maximum size comparable to the bottleneck radius. For the non-motile part of the life cycle, which also has the greatest metabolic needs, these colonies would just barely be able to obtain sufficient nutrients by diffusion alone.

Results: Flows, Advection, and Nutrient Uptake

How does advection, the transport of solutes by flow, modify this picture? The advection-diffusion equation

$$\frac{\partial C}{\partial t} + \vec{u} \cdot \vec{\nabla} C = D \nabla^2 C \quad (4)$$

gives the concentration field $C(\vec{r}, t)$, where \vec{u} is the fluid velocity. The standard measure of the competition between advection and diffusion is the (dimensionless) Peclet number,¹⁵ which can be expressed in terms of a typical flow velocity U and the sphere diameter $2R$ as

$$Pe = \frac{2RU}{D} . \quad (5)$$

Our recent measurements⁴ of the typical fluid velocity near *Volvox carteri* (Fig. 1E) have shown that Pe can range from 100 – 300, implying that long-range diffusion is negligible compared to advection. For large Pe , the absorption rate I_a generally is a power-law in Pe , as a consequence of the boundary layer that forms near the sphere’s surface. For the no-slip boundary condition at the surface of a solid sphere, Acrivos and Taylor¹⁶ showed that $I_a \sim RPe^{1/3}$ for large Pe . In important recent work, Magar, Goto, and Pedley^{17,18} found that the exponent changes when the boundary condition allows slip; with a prescribed tangential flow, the current is $I_a \sim RPe^{1/2}$. Since we seek the size dependence of the advective transport, we require a model of the flow field created by the flagella.

It is impractical to calculate the detailed flow generated by the array of flagella at the colony surface. Instead, we develop a simple model in which the details of the flagella length, beating frequency, and waveform are subsumed into a single averaged parameter, the force per

unit area \vec{f} that the spherical surface exerts on the fluid. Using the measured value of the propulsive thrust for *V. carteri*³ we estimate $f \simeq 0.1 \text{ dyne/cm}^2$, where we have divided the experimentally determined total thrust force by the area of a colony. Since we prescribe the force per unit area, the shear stress, instead of the tangential flow at the surface of the colony, our flow has crucial qualitative differences from previous work.^{17,18} Dimensional analysis shows that the characteristic magnitude of the flow velocity U grows with colony radius

$$U \sim \frac{fR}{\eta} \quad (6)$$

where $\eta = 0.01 \text{ g/cm-s}$ is the viscosity of water. When the tangential flow velocity is prescribed, the flow is clearly independent of R . In accord with observations³, our model predicts that larger colonies with the same average density swim faster than smaller ones. For example, using our estimate of f and a colony radius of $R = 100 \text{ }\mu\text{m}$ we find $U \sim 500 \text{ }\mu\text{m/s}$, which is close to observed swimming speeds.^{1,3,4}

For an idealized model, we take the force per unit area to be directed along lines of longitude, $\vec{f} = f\hat{\theta}$ (see Fig. 3 for coordinate system); it is straightforward to include an azimuthal component of \vec{f} to allow for rotational motion as well (M.B. Short, et al., unpublished) Thus, the boundary conditions at the surface of the colony are vanishing radial velocity and the shear stress condition $\sigma_{r\theta} = -f$, where $\sigma_{r\theta}$ is the stress that the fluid exerts on the surface. Far from the colony, the fluid velocity approaches the swimming velocity $\vec{U} = -U\hat{z}$, or zero, when the colony is held in place. With these boundary conditions, the Stokes equation $\vec{\nabla} p = \eta \nabla^2 \vec{u}$, is solved by an expansion in Legendre polynomials multiplying functions that are linear combinations of powers of r . In a coordinate system moving at the speed of the colony, the radial and polar velocities are $u_r = -U[(c-x^{-3})\cos\theta + A(x, \theta)]$ and $u_\theta = -U[-(d+x^{-3})\sin\theta + B(x, \theta)]$, where $x = r/R$ and $A(x, \theta)$ and $B(x, \theta)$ are infinite sums of terms falling off with distance as x^{-2} and higher powers. The precise characteristic velocity whose dimensional scaling was shown in Eq. 6 is found to be $U = \pi f R / 8\eta$. The parameters c and d distinguish between free-swimming colonies ($c = d = 1$) with no net force acting on them and colonies held in place by an anchoring force ($c = 1/x, d = 1/2x$).

To test this model, we measured the flow fields around colonies using methods described in detail elsewhere,⁴ building on earlier studies.^{19,20} and summarized in the Methods section. A least-squares fit of each data set was used to determine the velocity scale U for each, and then each data set was normalized by the maximum velocity. Pooling data on 10 colonies, Figure 3 shows this averaged velocity compared to the suitably normalized theoretical function; the two agree within the standard error of the measurements, validating the idea of surface shear stress supplied by the flagella.

We now examine in detail the nutrient uptake rate. Observe from Eq. 5 that since the flow field in the model has a characteristic velocity U that is proportional to the radius, the Peclet number is proportional to R^2 . Since the Peclet number itself is dimensionless, it can be expressed as the ratio of two radii in the form $Pe = (R/R_a)^2$ with

$$R_a = \sqrt{\frac{4\eta D}{\pi f}}. \quad (7)$$

In addition to the bottleneck radius R_b , this “advection radius” R_a serves as a second characteristic length scale in the system, one not previously recognized. It is the length above which advection overtakes diffusion, i.e. $Pe > 1$. With the estimated parameters described above, we find $R_a \sim 10\mu\text{m}$, slightly larger than the diameter of *Chlamydomonas*. The ratio $\Lambda \equiv R_b/R_a$ serves as a parameter characterizing the onset of complexity in the Volvocales, and is in the range 5 – 10. Note that R_a is comparable to the length of a flagellum, the “stirring rod,” certainly a curious coincidence.

To understand the role of the advection radius in the rate of molecular nutrient and waste exchange, we used the self-generated flow field calculated above as the ve-

locity \vec{u} in the steady-state version of Eq. 4 to find numerically the concentration profile around a model colony. Figure 4a shows the normalized concentration field C/C_∞ near a swimming colony for a range of Peclet numbers. When $Pe \sim 1$, the concentration field is only slightly distorted from spherical symmetry, while for $Pe \gg 1$, a thin concentration boundary layer forms around the leading edge of the sphere; furthermore, a solute plume, analogous to the “tail” behind sedimenting marine snow²², extends to ever greater length. This plume of nutrient depletion or waste product accumulation is left behind a swimming colony. As an increasing Peclet number is associated with increasing radius, we may imagine the three frames in Fig. 4a as corresponding to organisms small in comparison to the advective radius, comparable in size, and then much larger. Since R_a is the measure of the size of the boundary layer, the boundary layer width R_a/R , in units of the colony radius, is proportional to $Pe^{-1/2}$. Computations are consistent with this scaling (Fig. 4b), where the boundary layer thickness is taken to be the distance over which the scaled concentration $C/C_\infty = 0.1$ in front of the colony. The absorption current I_a follows from Fick’s law as an integral, $I_d = D \int dS(\partial C/\partial r)$, over S , the colony surface. We approximate $\partial C/\partial r \simeq C_\infty/R_a$ at the surface, yielding

$$I_a \simeq \frac{4\pi R^2 DC_\infty}{R_a}. \quad (8)$$

The right-hand-side of Eq. 8 may also be expressed as $4\pi DC_\infty RPe^{1/2}$, the same power law found by Magar, *et al.*,^{17,18} whose velocity field included only the first few Legendre polynomial terms. The key new point here is that the quadratic dependence of the Peclet number on radius (quite miraculously!) leads to a solute current that scales with the surface area, just as required. Figure 2b revisits the competition between pure diffusive current and metabolic needs first illustrated in Fig. 2a, but now presented on a log-log plot. It shows how the total molecular current crosses over from a diffusion-dominated linear behaviour for $R < R_a$ to advection-dominated quadratic scaling for $R > R_a$. This scaling is the same power as that for the metabolic needs. We therefore conclude that transport by the collective beating of flagella eliminates the diffusion-only inhibition of growth and thus the transition to multicellularity.

Discussion

Viewed from a different perspective, the flows we have described enhance the molecular or metabolite exchange rate *per unit area* of a colony. This advective contribution confers an advantage to increasing size, for it rises precipitously from the smallest organisms up to those whose size is several times the advection radius (Fig. 5). These results suggest that “a greater rate of nutrient acquisition per unit area” is one answer to the often-posed question

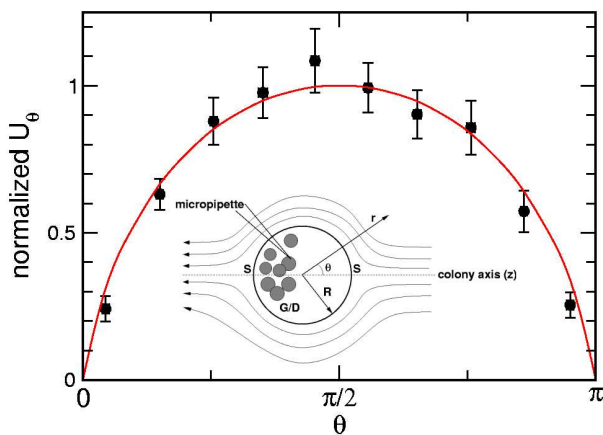


FIG. 3: Flow field near the surface of a colony. Inset shows geometry of the experiment. The organism is held fixed using a micropipette attached to the posterior region, in the vicinity of the germ cells/daughter colonies (G/D), away from the two stagnation points (S) of the flow. The fluid flow generated by the colony is measured using particle imaging velocimetry (PIV). Comparison between theoretical (red curve) and average experimental values (solid circles) of the tangential flow velocity near the organism’s surface is plotted as a function of polar angle θ . Measurements were made on ten different organisms. For each a least-squares fit to the theoretical velocity field was performed to determine the single unknown parameter, the maximum tangential velocity. These data were then pooled by normalizing each set to the fitted maximum velocity, ranging from 100 – 600 $\mu\text{m}/\text{s}$ for the colonies measured.

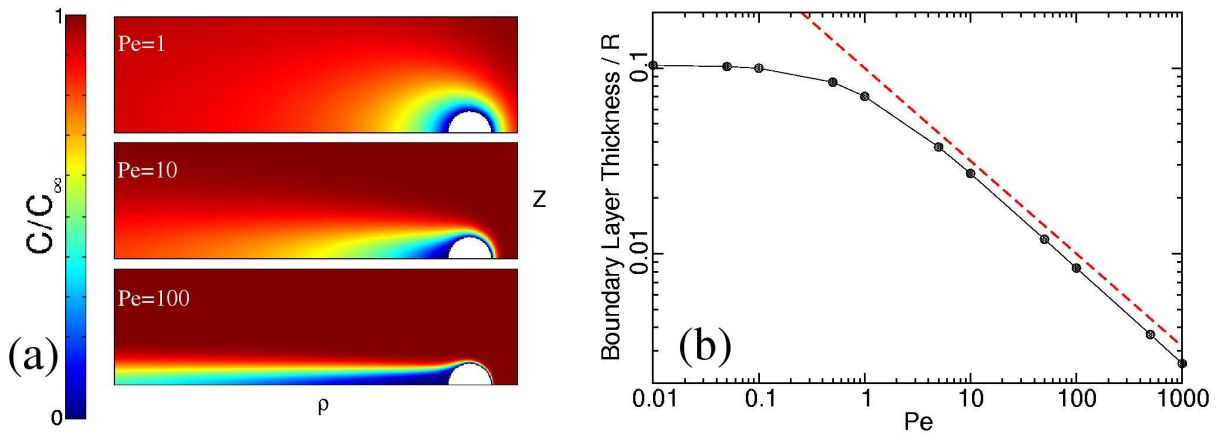


FIG. 4: Results from numerical calculations of spatial dependence of the concentration field using the theoretically obtained velocity field. (a) Concentration near a perfectly absorbing [$C(R) = 0$] swimming spherical colony for various Peclet numbers, illustrating the development of a thin localized anterior boundary layer and long narrow posterior plumes at high swimming speeds. Colors represent the dimensionless concentration (color bar at left). The concentration fields near an immobilized colony are quantitatively very similar. (b) The relationship between boundary layer thickness and Peclet number. The thickness was determined from the computations as the distance from the front surface of the sphere to the point at which $C/C_\infty = 0.1$. When displayed as shown on a log-log plot (black line), the boundary layer thickness, divided by sphere radius R , is parallel to a line (dashed red) proportional to $Pe^{-1/2}$, indicating that it also varies as the $-1/2$ power at Peclet numbers greatly exceed unity.

regarding the advantages of increased size,²³ particularly for colonial forms with only a few cells. Significantly, the levelling out of the exchange rate for even larger colonies implies size neutrality in that regime. Perhaps this contributes to the polyphyletic origin of the Volvocales.

While we have focused on the central issue of metabo-

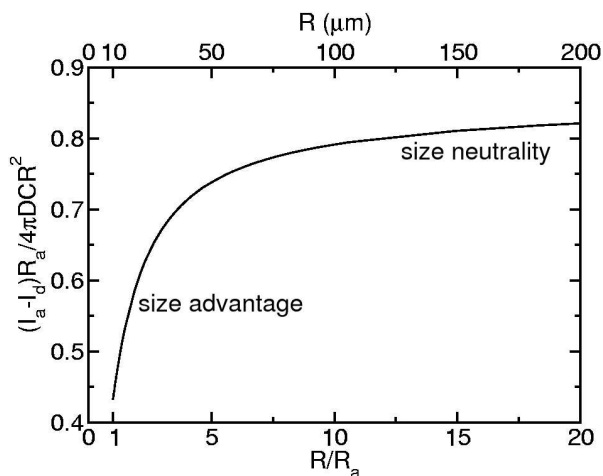


FIG. 5: Difference between molecular flux (current/area) with advection, and without, plotted as a function of the colony radius R , in units of the advective radius R_a . Numerical results derived, using flagella-driven flow, show that beyond R_a the advective contribution overpowers pure diffusion. Beyond $\sim 100 \mu\text{m} = 10 R_a$, the approximate size where germ/soma differentiation occurs in the Volvocales, that difference saturates, indicating the onset of size neutrality.

lite exchange in the presence of strong fluid transport by flagella, the solute plumes (Fig. 4a), representing either depletion and waste, also provide spatially and temporally extended signals for the presence of a colony, perhaps significant both for intercolony communication, as in sexual induction,²⁴ and for spatial patterning via chemotaxis. In the context of predation, a solute plume increases the probability of detection.

Methods

Colonies of *Volvox carteri f. nagariensis* harvested from synchronized populations grown in standard *Volvox* medium²¹ under controlled dark/light cycles (18 h light, 1000 foot-candles, 28° C/6 h dark, 26° C) are held fixed by micropipette aspiration (Fig. 2), viewed at 4× magnification on the stage of an inverted microscope (Nikon Diaphot 200). Movies were acquired with an analog ccd camera (Sony SSC-M374, 480 × 640 pixels) and were typically composed of ~ 1000 images taken at ~ 30 frames/s. The resulting flow fields were smoothed by averaging over > 200 frames. For particle imaging velocimetry (PIV) studies the medium was seeded with microspheres (Molecular Probes, F8825 carboxylate modified, 1.0 μm , Nile red), viewed using laser epifluorescence (80 mW, 532 nm) or darkfield illumination. Commercial PIV software (Dantec Dynamics, Skovlunde, Denmark) was used. Averaged velocity fields were used to obtain the tangential velocity component as a function of polar angle θ (Fig. 2), with typically 20 measurements between $\theta = 0$ and $\theta = \pi$. Apart from minor distortions due to the micropipette, symmetry between the two halves of the profile was observed; we combined those data and

partitioned them into 10 bins.

We are grateful to H.C. Berg, T.E. Huxman, R.E. Michod, R. Stocker, and especially to A.M. Nedelcu for important discussions and to L. Cisneros, C. Dombrowski, and C. Smillie for experimental assistance. This work was supported in part by NSF grants DEB-0075296 (CAS), PHY-0551742 (MBS,SG,JOK,REG), and CMS-0093658 (TRP).

-
- [1] Niklas, K.J. (1994) *Plant Allometry* (University of Chicago Press, Chicago).
- [2] Kirk, D.L. (1998) *Volvox: Molecular-Genetic Origins of Multicellularity and Cellular Differentiation* (Cambridge University Press, Cambridge).
- [3] Solari, C.A. (2005) Ph.D. Dissertation, University of Arizona.
- [4] Solari, C.A., Ganguly, S., Michod, R.E., Kessler, J.O. & Goldstein, R.E. (2006) *Proc. Natl. Acad. Sci. USA* **103**, 1353-1358.
- [5] Koufopanou, V. (1994) *Amer. Nat.* **143**, 907-931.
- [6] Larson, A., Kirk, M.M. & Kirk, D.L. (1992) *Mol. Biol. Evol.* **9**, 85-105.
- [7] Coleman, A.W. (1999) *Proc. Natl. Acad. Sci. USA* **96**, 13892-13897.
- [8] Nozaki, H., Ohta, N., Takano, H. & Watanabe, M.M. (1999) *J. Phycol.* **35**, 104-112.
- [9] Nozaki, H. (2003) *Biologia* **58**, 425-431.
- [10] Bell, B. (1985) in *The Origin and Evolution of Sex*, H.O. Halvorson and A. Monroy, eds. (Alan R. Liss, Inc., New York), p. 221.
- [11] Koufopanou, V. & Bell, G. (1993) *Proc. Roy. Soc. London B, Biol. Sci.* **254**, 107-113.
- [12] Berg, H.C. & Purcell, E.M. (1977) *Biophys. J.* **20**, 193-219.
- [13] Senft, W.H., Hunchberger, R.A. & Roberts, K.E. (1981) *J. Phycol.* **17**, 323-329.
- [14] King, N. (2004) *Develop. Cell* **7**, 313-325.
- [15] Guyon, E., Hulin, J.P., Petit, L. & Mitescu, C.D. (2001) *Physical Hydrodynamics* (Oxford University Press, Oxford).
- [16] Acrivos, A. & Taylor, T.D. (1962) *Phys. Fluids* **5**, 387-394.
- [17] Magar, V., Goto, T. & Pedley, T.J. (2003) *Q. J. Mech. Appl. Math.* **56**, 65-91.
- [18] Magar, V. & Pedley, T.J. (2005) *J. Fluid Mech.* **539**, 93-112.
- [19] Hand, W.G. & Haupt, W. (1971) *J. Protozool.* **18**, 361-364.
- [20] Hiatt, J.D.F. & Hand, W.G. (1972) *J. Protozool.* **19**, 488-489.
- [21] Kirk, D.L. & Kirk, M.M. (1983) *Dev. Biol.* **96**, 493-506.
- [22] Kjørboe, T. & Jackson, G.A. (2001) *Limnol. Oceanogr.* **46**, 1309-1318.
- [23] Bonner, J.T. (1998) *Integr. Biol.* **1**, 27-36.
- [24] Nedelcu, A.M., Marcu, O. & Michod, R.E. (2004) *Proc. R. Soc. Lond. B* **271**, 1591-1596.